

## Preparation of $\text{SiO}_2$ -Coated $\text{TiO}_2$ Composite Materials with Enhanced Photocatalytic Activity Under UV Light

Shaozheng Hu,\* Fayun Li, and Zhiping Fan

Institute of Eco-environmental Sciences, Liaoning Shihua University, Fushun 113001, PR China

\*E-mail: hushaozheng001@163.com

Received January 13, 2012, Accepted March 6, 2012

$\text{SiO}_2$ -coated  $\text{TiO}_2$  composite materials with enhanced photocatalytic activity under UV light was prepared by a simple catalytic hydrolysis method. XRD, TEM, UV-vis spectroscopy, Photoluminescence, FT-IR and XP spectra were used to characterize the prepared samples. The obvious shell-core structure was shown for obtained  $\text{SiO}_2@\text{TiO}_2$  sample. The average thickness of the  $\text{SiO}_2$  coating layer was 2–3 nm. The interaction between  $\text{SiO}_2$  and  $\text{TiO}_2$  restrained the recombination of excited electrons and holes. The photocatalytic activities were tested in the degradation of an aqueous solution of a reactive dyestuff, methylene blue, under UV light. The photocatalytic activity of  $\text{SiO}_2@\text{TiO}_2$  was much higher than that of P25 and mechanical mixing sample  $\text{SiO}_2/\text{TiO}_2$ . The possible mechanism for the photocatalysis was proposed.

**Key Words :**  $\text{TiO}_2$ , Photocatalysis,  $\text{SiO}_2$ , Coating, UV light

### Introduction

The past decades have witnessed growing interest in an advanced oxidation technique-heterogeneous photocatalysis, for wastewater treatment and water purification.<sup>1</sup>  $\text{TiO}_2$ , as a common photocatalysis, is widely used for the mineralization of environmental pollutants including organic or inorganic and it exhibits strong oxidation activity under ultraviolet light. The photocatalysis process can decompose many organic compounds, especially trace organics, to carbon dioxide, water, and mineral ions. Although the utilization of nanosized  $\text{TiO}_2$  catalyst has attracted a great deal of attention due to their high photocatalytic reactivity, the actual factors affecting the photocatalytic activity of  $\text{TiO}_2$  particles are still unclear. Besides, the high rate of recombination between excited electron and hole result in a low quantum yield rate and also a limited photooxidation rate.<sup>1</sup>

$\text{SiO}_2$ , as a kind of good carrier, has been widely used in the material synthesis field. In recent years, titania-silica composite materials have been widely investigated, and in most cases these catalysts show a higher photocatalytic activity than the neat  $\text{TiO}_2$  prepared in parallel for the oxidation of organic pollutants in water.<sup>2–5</sup>  $\text{SiO}_2$  was believed to be a very good medium, which not only facilitates adsorbing organics and transfers those adsorbed compounds to active sites on  $\text{TiO}_2$ ,<sup>6</sup> but also benefits to the dispersion of the  $\text{TiO}_2$  particles.<sup>7</sup> Besides, it is also reported that  $\text{SiO}_2$  modification is effective to separate the photogenerated electrons and holes which is of great importance for the photocatalytic activity. Moreover,  $\text{SiO}_2/\text{TiO}_2$  shell-core structure particles exhibit novel properties that are not found in either single oxide.

Many strategies for preparing titania-silica materials, such as catalytic hydrolysis,<sup>8</sup> grafting of titanium alkoxides on the  $\text{SiO}_2$  surface,<sup>9</sup> coprecipitation,<sup>10</sup> impregnation,<sup>11</sup> and chemical

vapor deposition,<sup>12</sup> have been proposed more recently. In this paper,  $\text{SiO}_2$ -coated  $\text{TiO}_2$  composite materials with enhanced photocatalytic activity under UV light was prepared by a simple catalytic hydrolysis method using  $\text{Na}_2\text{SiO}_3$  as silicon source. The photocatalytic activities were tested in the degradation of an aqueous solution of a reactive dyestuff, methylene blue, under UV light. The possible mechanism for the photocatalysis was proposed.

### Experimental

**Preparation and Characterization.** 50 g of P25 were ultrasonically treated in 500 mL of water for 30 min to obtain a well-dispersed  $\text{TiO}_2$  suspension. This suspension was transferred into a 2000 mL flask, kept in a water bath, and heated to 80 °C. The pH value was adjusted to 10 by adding NaOH (0.1 mol/L) aqueous solution. Aqueous solution of  $\text{Na}_2\text{SiO}_3$  (0.5 mol/L) was added dropwise to the  $\text{TiO}_2$  suspension. The pH value of the reaction solution was kept constant during the coating process by adding  $\text{H}_2\text{SO}_4$  (0.1 mol/L) dropwise. The final mole ratio of  $\text{TiO}_2$  to  $\text{Na}_2\text{SiO}_3$  is 5. After feeding, the obtained suspension was aged for 3 h. The precipitate was filtrated and washed with distilled water for 3 times. Then the washed precipitate was dried at 110 °C for 3 h, and calcined at 400 °C for 2 h. The obtained sample was denoted as  $\text{SiO}_2@\text{TiO}_2$ . For comparison, mechanical mixing sample with the same mole ratio of  $\text{TiO}_2$  to  $\text{Na}_2\text{SiO}_3$  is prepared. The obtained mixture was calcined at 400 °C for 2 h, and denoted as  $\text{SiO}_2/\text{TiO}_2$ .

XRD patterns of the prepared  $\text{TiO}_2$  samples were recorded on a Rigaku D/max-2400 instrument using Cu-K $\alpha$  radiation ( $\lambda = 1.54 \text{ \AA}$ ). TEM images were measured using a Philips Tecnai G220 model microscope. UV-vis spectroscopy measurement was carried out on a JASCO V-550 model UV-vis spectrophotometer, using  $\text{BaSO}_4$  as the reflectance sample.

XPS measurements were conducted on a Thermo Escalab 250 XPS system with Al K $\alpha$  radiation as the exciting source. The binding energies were calibrated by referencing the C 1s peak (284.6 eV) to reduce the sample charge effect. Photoluminescence (PL) spectra were measured at room temperature with a fluorospectrophotometer (FP-6300) using an Xe lamp as excitation source.

**Photocatalytic Reaction.** Methylene blue (MB) was selected as model compound to evaluate the photocatalytic performance of the prepared TiO<sub>2</sub> particles in an aqueous solution under visible light irradiation. 0.1 g TiO<sub>2</sub> powders were dispersed in 100 mL aqueous solution of MB (initial concentration  $C_0 = 50$  ppm) in an ultrasound generator for 10 min. The suspension was transferred into a self-designed glass reactor, and stirred for 30 min in darkness to achieve the adsorption equilibrium. The concentration of MB at this point was considered as the absorption equilibrium concentration  $C_0$ . The adsorption capacity of a catalyst to MB was defined by the adsorption amount of MB on the photocatalyst ( $C_0 - C_0'$ ). In the investigation of photodegradation by UV light, a 125 W high-pressure mercury lamp with a water cooling cylindrical jacket was used. All runs were conducted at ambient pressure and 30 °C. At given time intervals, 4 mL suspension was taken and immediately centrifuged to separate the liquid samples from the solid catalyst. The concentrations of MB before and after reaction were measured by means of a UV-Vis spectrophotometer at a wavelength of 665 nm. The percentage of degradation  $D\%$  was determined as follows:

$$D\% = \frac{A_0 - A}{A_0} \times 100\% \quad (1)$$

Where  $A_0$  and  $A$  are the absorbances of the liquid sample before and after degradation, respectively.

## Results and Discussion

The XRD patterns of prepared samples (Fig. 1) indicated that all TiO<sub>2</sub> samples were mixture of anatase and rutile phases. The phase contents of the samples were estimated from their XRD patterns by the following equation<sup>13</sup>

$$x_A = \frac{1}{1 + 1.26 \times \frac{I_R}{I_A}} \quad (2)$$

where  $x_A$  is the fraction of anatase phase,  $I_R$  and  $I_A$  are the intensities of the anatase (101) and rutile (110) diffraction peaks, respectively. The contents of anatase phase in SiO<sub>2</sub>@TiO<sub>2</sub>, SiO<sub>2</sub>/TiO<sub>2</sub>, and P25 were 74.2, 74.7, and 74.1, respectively. This indicates that preparation method did not influence the phase content. However, as shown in Figure 1, the peak intensities of SiO<sub>2</sub>@TiO<sub>2</sub> and SiO<sub>2</sub>/TiO<sub>2</sub> were obviously lower than that of P25. This is not attributed to the decreased particle size but the coverage of SiO<sub>2</sub> on the TiO<sub>2</sub> surface which decrease the diffraction intensity.

Figure 2 shows the representative TEM (left) and HRTEM

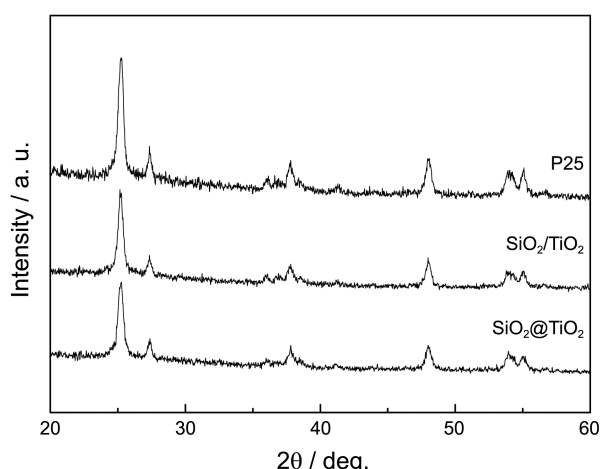


Figure 1. XRD patterns of P25 and the prepared samples.

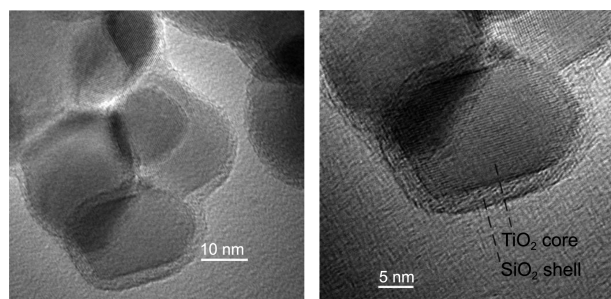


Figure 2. TEM (left) and HRTEM (right) of SiO<sub>2</sub>@TiO<sub>2</sub>.

(right) of SiO<sub>2</sub>@TiO<sub>2</sub>. The obvious shell-core structure was shown for SiO<sub>2</sub>@TiO<sub>2</sub>, indicating the homogeneous coverage happened between SiO<sub>2</sub> and TiO<sub>2</sub> (Fig. 2, left). In the HRTEM (right), the ordered crystal lattices and amorphous structure were shown in the core and shell of SiO<sub>2</sub>@TiO<sub>2</sub>, respectively. This indicated the core and shell of SiO<sub>2</sub>@TiO<sub>2</sub> was TiO<sub>2</sub> and SiO<sub>2</sub>, respectively. The SiO<sub>2</sub>-coated TiO<sub>2</sub> was obtained. It is shown in the HRTEM that the average thickness of the SiO<sub>2</sub> coating layer was 2-3 nm.

It is known that the absorption of light influences the photocatalytic activity significantly. Figure 3 shows the UV-

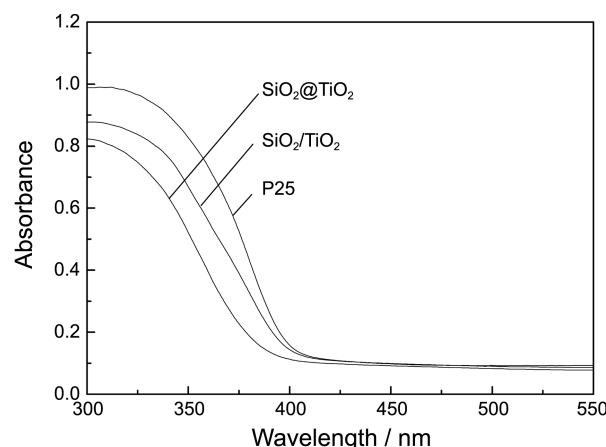
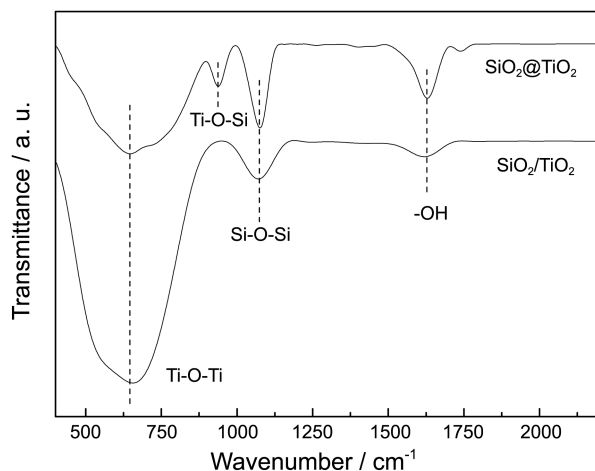


Figure 3. UV-vis diffuse reflectance spectra of P25 and the prepared samples.



**Figure 4.** FT-IR spectra of prepared  $\text{SiO}_2/\text{TiO}_2$  and  $\text{SiO}_2@\text{TiO}_2$ .

vis spectra of P25 and prepared samples. The absorption edges around 400 nm were observed for all the samples. No absorption in visible light region was shown for all the samples. Besides, it is denoted that the absorption in UV light region decreased for  $\text{SiO}_2/\text{TiO}_2$  and  $\text{SiO}_2@\text{TiO}_2$  compared with P25 sample. This is probably due to the coverage of  $\text{SiO}_2$  on  $\text{TiO}_2$  surface restrained the absorption of UV light.

Figure 4 shows the FT-IR spectra of prepared  $\text{SiO}_2/\text{TiO}_2$  and  $\text{SiO}_2@\text{TiO}_2$ . The bands at 650, 1080, and 1640  $\text{cm}^{-1}$  were observed in the spectra of  $\text{SiO}_2/\text{TiO}_2$  and  $\text{SiO}_2@\text{TiO}_2$ . The band around 650  $\text{cm}^{-1}$  attributes to the Ti-O-Ti stretching vibration of crystalline  $\text{TiO}_2$  phase.<sup>14</sup> The band near 1080  $\text{cm}^{-1}$  corresponds to the asymmetric stretching vibration of Si-O-Si bond.<sup>15</sup> The bands at around 1640  $\text{cm}^{-1}$  is attributed to the bending vibration of hydroxyl groups. Besides, another band which around 930  $\text{cm}^{-1}$  is shown in the spectrum of  $\text{SiO}_2@\text{TiO}_2$  sample but not in that of  $\text{SiO}_2/\text{TiO}_2$ . This FT-IR band is commonly accepted as the characteristic stretching vibration of Ti-O-Si bonds in Ti- and Si-containing catalysts,<sup>16</sup> which implies that the substitution of Si for Ti occurred to form Si-O-Ti bonds in  $\text{SiO}_2@\text{TiO}_2$  sample.

XPS is an effective surface test technique for characterizing elemental composition and chemical states. The binding energy of the element is influenced by its electron density. An increase of binding energy implies the lowering of the electron density. In the region of Ti 2p (Fig. 5(a)), the binding energy of P25 and  $\text{SiO}_2/\text{TiO}_2$  were 458.6 eV (Ti-O-Ti bond), indicating the chemical environment of two samples are the same. However, for  $\text{SiO}_2@\text{TiO}_2$  sample, the binding energy increased to 458.9 eV, indicating the decreased electron densities on Ti atoms compared with other two samples. This is probably attributed to the formation of Ti-O-Si bond in  $\text{SiO}_2@\text{TiO}_2$  sample.<sup>17</sup> Due to the higher electronegativity of oxygen, the electrons will be transferred from titanium and silicon to oxygen. Si can supply less electrons than Ti in Ti-O-Si bond. Therefore, compared with Ti-O-Ti bond, more electrons will be transferred from titanium to oxygen in Ti-O-Si bond, leading to the decreased electron densities on Ti atoms.

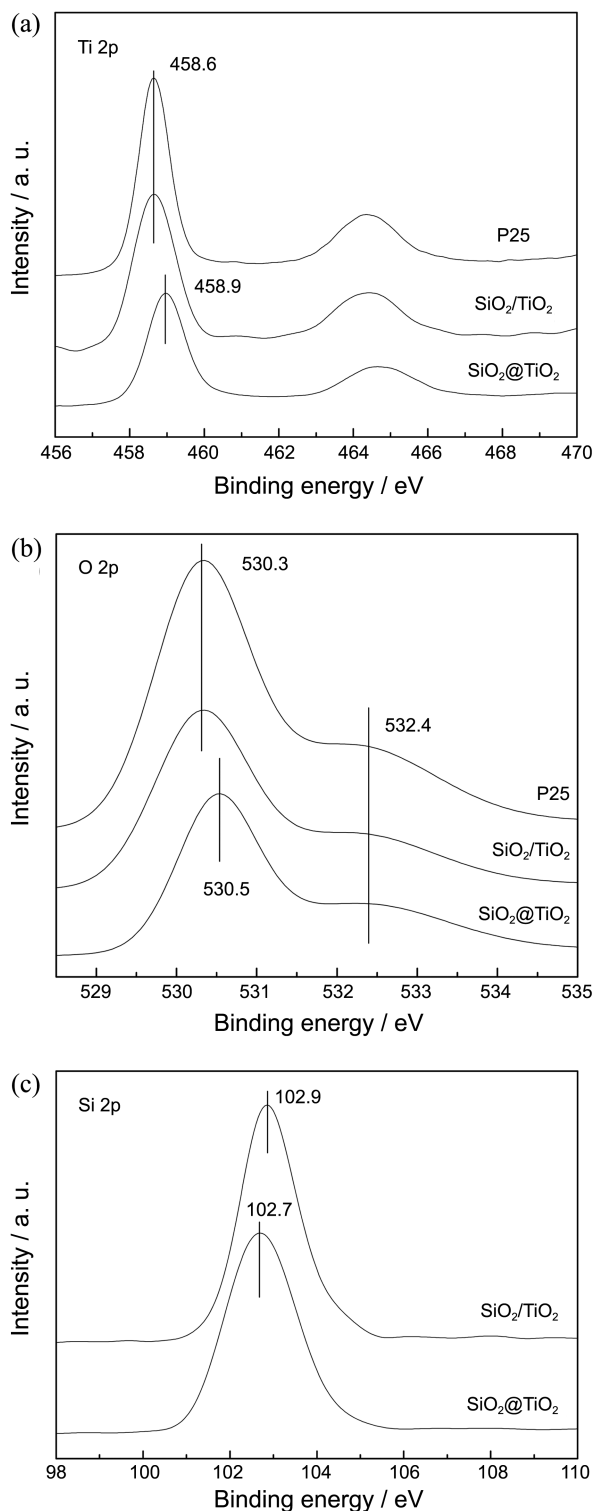


**Figure 5.** XP spectra of P25 and prepared samples in the region of Ti 2p (a), O 2p (b), and Si 2p (c).

In the region of O 2p (Fig. 5(b)), the similar trend was shown. The binding energy of P25 and  $\text{SiO}_2/\text{TiO}_2$  were the same (530.3 eV), but increased to 530.5 eV for  $\text{SiO}_2@\text{TiO}_2$  sample. Compared with Ti, Si can transfer less electrons to O in Ti-O-Si bond, leading to the decreased electron densities and high binding energy of O atoms. In the region of Si

2p (Fig. 5(c)), the binding energy of  $\text{SiO}_2/\text{TiO}_2$  was 102.9 eV which attributed to the Si-O-Si bond.<sup>18</sup> For  $\text{SiO}_2@\text{TiO}_2$  sample, this binding energy decreased to 102.7 eV, which is probably due to the presence of Si-O-Ti bond. Compared with Si-O-Si bond, more electrons will be transferred from Ti to O in Si-O-Ti bond, leading to the increased electron densities on Si atoms. Therefore, the binding energy of Si 2p in  $\text{SiO}_2@\text{TiO}_2$  sample was lower than that of  $\text{SiO}_2/\text{TiO}_2$  sample. In conclusion, it is deduced from XP spectra that not the mechanical mixing but some interaction existed between  $\text{SiO}_2$  and  $\text{TiO}_2$  in  $\text{SiO}_2@\text{TiO}_2$ .

Besides, the surface O/(Ti+Si) ratios of P25,  $\text{SiO}_2/\text{TiO}_2$ , and  $\text{SiO}_2@\text{TiO}_2$  were calculated from XPS spectra. The results showed that the O/(Ti+Si) ratios of P25,  $\text{SiO}_2/\text{TiO}_2$ , and  $\text{SiO}_2@\text{TiO}_2$  were 1.98, 1.99, and 1.82, respectively. Liu *et al.*<sup>19</sup> suggested that there existed oxygen vacancy when this ratio was lower than 2.0. Such oxygen vacancies will give rise to the formation of a defect level which acts as the hole-traps to reduce the recombination of excited electrons and holes, thus promote the charge transfer.<sup>20</sup>

PL emission spectrum, which is closely related to surface states and stoichiometric chemistry, is used to determine the efficiency of trapping, migration, and transfer of a charge carrier, and to understand the fate of electron-hole pairs in semiconductors. Figure 6 shows the PL spectra of P25 and prepared samples using excitation at 300 nm. The PL intensity of  $\text{SiO}_2/\text{TiO}_2$  was slightly decreased compared with P25. However, for  $\text{SiO}_2@\text{TiO}_2$ , the PL intensity was obviously decreased. As the PL emission is the result of the recombination of excited electrons and holes, the lower PL intensity indicates the decrease in recombination rate, thus higher photocatalytic activity.<sup>21</sup> Therefore, it is deduced that the interaction existed between  $\text{SiO}_2$  and  $\text{TiO}_2$  in  $\text{SiO}_2@\text{TiO}_2$ , which cause the formation of the oxygen vacancy, thus lead to the reduced recombination of excited electrons and holes. This is consistent with the XPS results.

The adsorption of MB on  $\text{TiO}_2$ -based catalysts was measured by the equilibrium adsorption capacity and shown in Figure 7. It is indicated that the adsorption capacity

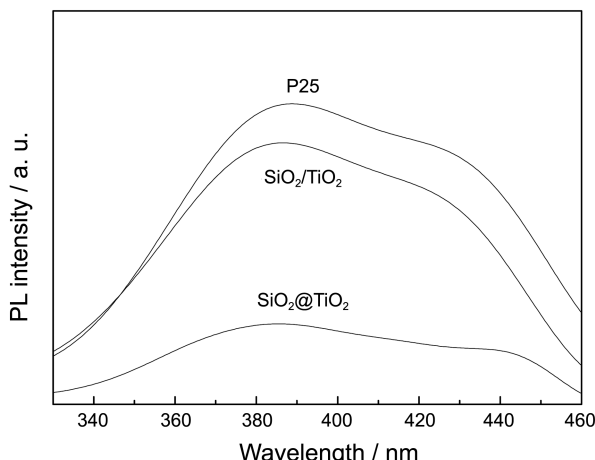


Figure 6. Photoluminescence emission spectra of P25 and the prepared catalysts.

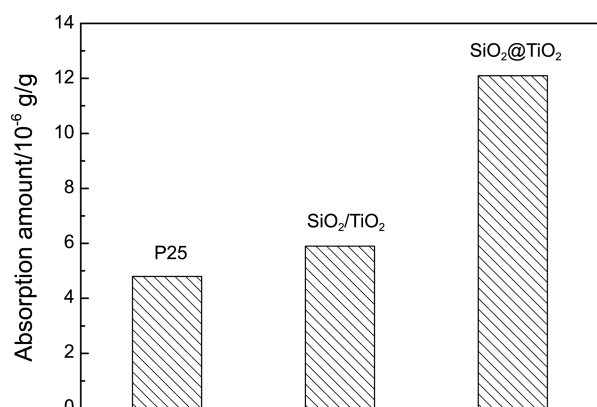


Figure 7. Adsorption capacity of MB on P25 and the prepared catalysts.

increased slightly when P25 mechanical mixing with  $\text{SiO}_2$  ( $\text{SiO}_2/\text{TiO}_2$ ) compared with P25 alone. However, for  $\text{SiO}_2@\text{TiO}_2$  sample, an obvious improvement of adsorption capacity was observed. More than 24% MB was adsorbed on the  $\text{SiO}_2@\text{TiO}_2$  surface, which is 2.5 times of P25. This indicated that  $\text{SiO}_2$  modification can improve the adsorption capacity of  $\text{TiO}_2$  catalyst.<sup>22</sup> Besides, the obvious difference in adsorption capacity between  $\text{SiO}_2/\text{TiO}_2$  and  $\text{SiO}_2@\text{TiO}_2$  hint that not the mechanical mixing but some interaction existed between  $\text{SiO}_2$  and  $\text{TiO}_2$  in  $\text{SiO}_2@\text{TiO}_2$ , which is consistent with the XPS and PL result.

The photocatalytic activities of P25 and prepared samples under UV light are shown in Figure 8. Without light or catalyst, almost no MB was degraded after 60 min, indicating that the contribution of self-degradation was negligible. The P25 exhibited poor activity. The mechanical mixing sample  $\text{SiO}_2/\text{TiO}_2$  showed slightly lower activity than that of P25. This is probably due to the low absorption in UV light region of  $\text{SiO}_2/\text{TiO}_2$  compared with P25, leading to the lower UV light utilization. However,  $\text{SiO}_2@\text{TiO}_2$  exhibited much higher photocatalytic activity than P25 and  $\text{SiO}_2/\text{TiO}_2$ . Approximately 90% MB were degraded after 60 min. The UV-vis result indicated that  $\text{SiO}_2@\text{TiO}_2$  exhibited the lowest

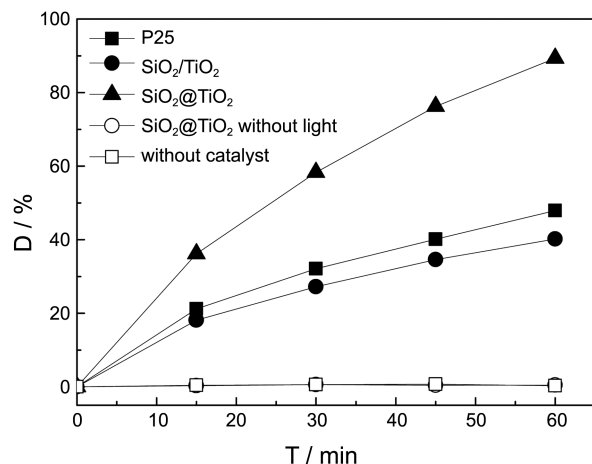


Figure 8. Photocatalytic activities of P25 and the prepared samples under UV light.

UV light absorption among the three samples, which is negative to the activity. Therefore, the outstanding photocatalytic activity of  $\text{SiO}_2@\text{TiO}_2$  must be due to the following two reasons: the increased adsorption of organic substrate and the low recombination rate of photogenerated electrons and holes which has been proved by PL spectra. The increased adsorption of organic substrate is favorable to the activity because the substrate adsorption is the precondition of photocatalysis. For  $\text{SiO}_2@\text{TiO}_2$  sample,  $\text{SiO}_2$  coated on  $\text{TiO}_2$  surface (Fig. 2), which caused the interaction between each other. Such interaction improved the separation rate of photogenerated electrons and holes, thus leading to the high activity.

### Conclusion

$\text{SiO}_2$ -coated  $\text{TiO}_2$  composite materials with enhanced photocatalytic activity under UV light was prepared by a catalytic hydrolysis method using  $\text{Na}_2\text{SiO}_3$  as silicon source. The XRD result indicated that there were no obvious changes in phase composition among the obtained samples. The obvious shell-core structure was shown for  $\text{SiO}_2@\text{TiO}_2$  sample. The average thickness of the  $\text{SiO}_2$  coating layer was 2–3 nm. XPS, FT-IR, and PL results indicated that not the mechanical mixing but some interaction existed between  $\text{SiO}_2$  and  $\text{TiO}_2$  in  $\text{SiO}_2@\text{TiO}_2$ .  $\text{SiO}_2@\text{TiO}_2$  exhibited much higher photocatalytic activity than P25 and  $\text{SiO}_2/\text{TiO}_2$  under UV light. Such outstanding photocatalytic activity of  $\text{SiO}_2@\text{TiO}_2$  was attributed to the increased adsorption of organic substrate and the low recombination rate of photo-generated electrons and holes.

**Acknowledgments.** This work was supported by National Natural Science Foundation of China (No. 41071317, 30972418), National Key Technology R & D Programme of China (No. 2007BAC16B07), the Natural Science Foundation of Liaoning Province (No. 20092080).

### References

1. Hoffmann, M. R.; Martin, S. T.; Choi, W.; Bahnemann, D. W. *Chem. Rev.* **1995**, *95*, 69.
2. Zou, J.; Gao, J. C. *J. Hazard. Mater.* **2011**, *185*, 710.
3. Obuchi, E.; Sakamoto, T.; Nakano, K. *Chem. Eng. Sci.* **1999**, *54*, 1525.
4. Anderson, C.; Bard, A. J. *J. Phys. Chem.* **1995**, *99*, 9882.
5. Bui, D. N.; Kang, S. Z.; Li, X. Q.; Mu, J. *Catal. Commun.* **2011**, *13*, 14.
6. Minero, C.; Catozzo, F.; Pelizzetti, E. *Langmuir* **1992**, *8*, 481.
7. Cheng, S.; Tsai, S. J.; Lee, Y. F. *Catal. Today* **1995**, *26*, 87.
8. Xu, Y.; Zheng, W.; Liu, W. *J. Photochem. Photobiol. A: Chem.* **1999**, *122*, 57.
9. Cozzolino, M.; Di Serio, M.; Tesser, R.; Santacesaria, E. *Appl. Catal. A: Gen.* **2007**, *325*, 256.
10. Doolin, P. K.; Alerasool, S.; Zalewski, D. J.; Hoffman, J. F. *Catal. Lett.* **1994**, *25*, 209.
11. Fernandez, A.; Caballero, A.; Gonzalez-Elipe, A. R. *Surf. Interf. Anal.* **1992**, *18*, 392.
12. Haukka, S.; Lakomaa, E.; Root, A. *J. Phys. Chem.* **1993**, *97*, 5085.
13. Hu, S. Z.; Wang, A. J.; Li, X.; Löwe, H. *J. Phys. Chem. Solids* **2010**, *71*, 156.
14. Lee, J. W.; Kong, S.; Kim, W. S.; Kim, J. *Mater. Chem. Phys.* **2007**, *106*, 39.
15. Yan, X. L.; He, J.; Evans, D. G.; Duan, X.; Zhu, Y. X. *Appl. Catal. B* **2005**, *55*, 243.
16. Khomane, R. B.; Kulkarni, B. D.; Paraskar, A.; Sainkar, S. R. *Mater. Chem. Phys.* **2002**, *76*, 99.
17. Liu, Y. M.; Ge, C.; Ren, M.; Yin, H. B.; Wang, A. L.; Zhang, D. Z.; Liu, C. Y.; Chen, J.; Feng, H.; Yao, H. P.; Jiang, T. S. *Appl. Surf. Sci.* **2008**, *254*, 2809.
18. Koshizaki, N.; Umebara, H.; Oyama, T. *Thin Solid Films* **1998**, *325*, 130.
19. Liu, B. S.; Wen, L. P.; Zhao, X. J. *Sol. Energy Mater. Sol. Cells* **2008**, *92*, 1.
20. Li, F. B.; Li, X. Z.; Hou, M. F.; Cheah, K. W.; Choy, W. C. H. *Appl. Catal. A* **2005**, *285*, 181.
21. Hu, S. Z.; Wang, A. J.; Li, X.; Wang, Y.; Löwe, H. *Chem. Asian J.* **2010**, *5*, 1171.
22. Bellardita, M.; Addamo, M.; Di Paola, A.; Marci, G.; Palmisano, L.; Cassar, L.; Borsa, M. *J. Hazard. Mater.* **2010**, *174*, 707.